Boosted Tree Classifier for in Vivo Identification of Early Cervical Cancer using Multispectral Digital Colposcopy

Nilgoon Zarei[1], Dennis Cox[2], Pierre Lane[1], Scott Cantor[3], Neely Atkinson[2], Jose-Miguel Yamal[4], Leonid Fradkin[5], Daniel Serachitopol[2], Sylvia Lam[1], Dirk Niekerk[6], Dianne Miller[7], Jessica McAlpine[7], Kayla Castaneda[5], Felipe Castaneda[5], Michele Follen[5] and Calum MacAulay[1]

[1]*Integrative Oncology, BC Cancer Research Centre and University of British Columbia, Vancouver, British Columbia, Canada*

[2]*Rice University, Houston, U.S.A.*

[3]*University of Texas, MD Anderson Cancer Center, Houston, U.S.A.*

[4]*University of Texas, Houston, U.S.A.*

[5]*Brookdale Hospital and Medical Center, New York, U.S.A.*

[6]*BC Cancer Agency, Vancouver, Canada*

[7]*Vancouver General Hospital, Vancouver, Canada*

Keywords: Boosted Tree Classifier, Machine Learning, Image Processing, Multispectral Digital Colposcopy, Cervical Cancer.

Abstract: Background: Cervical cancer develops over several years; screening and early diagnosis have decreased the incidence and mortality threefold over the last fifty years. Opportunities for the application of imaging and automation in the screening process exist in settings where resources are limited. Methods: Patients with high-grade squamous intraepithelial lesions (SIL) underwent imaging with a Multispectral Digital Colposcopy (MDC) prior to have a loop excision of the cervix. The image taken with white light was annotated by a clinician. The excised specimen was mapped by the study histopathologist blinded to the MDC data. This map was used to define areas of high grade in the excised tissue. Eleven reviewers mapped the histopathologic data into the MDC images. The reviewers' maps were analyzed and areas of agreement were calculated. We compared the result of a boosted tree classifier with a previously developed ensemble classifier. Results: Using a boosted tree classifier we obtained a sensitivity of 95%, a specificity of 96%, and an accuracy of 96% on the training sets. When we applied the classifier to a test set, we obtained a sensitivity of 82%, a specificity of 81%, and an accuracy of 81%. The boosted tree classifier performed better than the previously developed ensemble classifier. Conclusion: Here we presented promising results which show that a boosted tree analysis on MDC images is a method that could be used as an adjunct to colposcopy and would result in greater diagnostic accuracy compared to existing methods.

1 INTRODUCTION

Cervical cancer is a preventable disease. However, approximately 500,000 patients with cervical cancer are diagnosed every year and about half that many succumb to the disease. Cervical cancer has decreased in incidence and mortality in all countries with organized screening and detection programs. These programs are costly and require a great deal of trained personnel. Automated detection of cervical cancer and its precursors could improve cancer management in low and middle income countries where resources do not permit large screening infrastructure (world cancer research, 2012).

Cervical intraepithelial neoplasia (CIN) or SIL are cervical cancer precursors which can develop over three to twenty years into cancer. This long transition period makes cervical cancer an ideal cancer for early detection and treatment. Optical technologies such as fluorescence and reflectance spectroscopy have been extensively investigated as effective and non-invasive methods for cancer

Zarei N., Cox D., Lane P., Cantor S., Atkinson N., Yamal J., Fradkin L., Serachitopol D., Lam S., Niekerk D., Miller D., McAlpine J., Castaneda K., Castaneda F., Follen M. and MacAulay C. Boosted Tree Classifier for in Vivo Identification of Early Cervical Cancer using Multispectral Digital Colposcopy.
DOI: 10.5220/0006148900850091
In *Proceedings of the 10th International Joint Conference on Biomedical Engineering Systems and Technologies (BIOSTEC 2017)*, pages 85-91
ISBN: 978-989-758-215-8
Copyright © 2017 by SCITEPRESS – Science and Technology Publications, Lda. All rights reserved

A

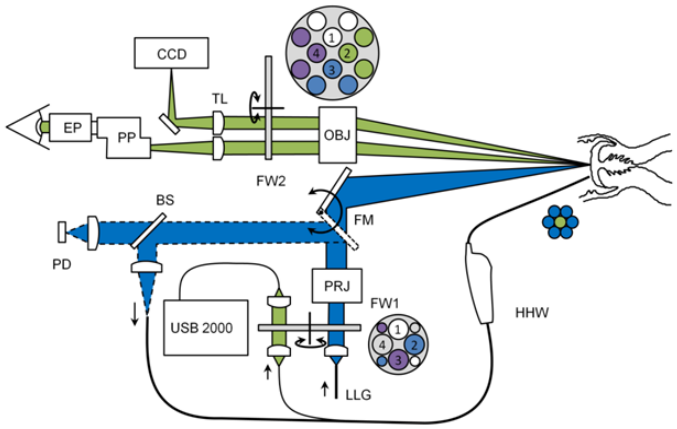

B

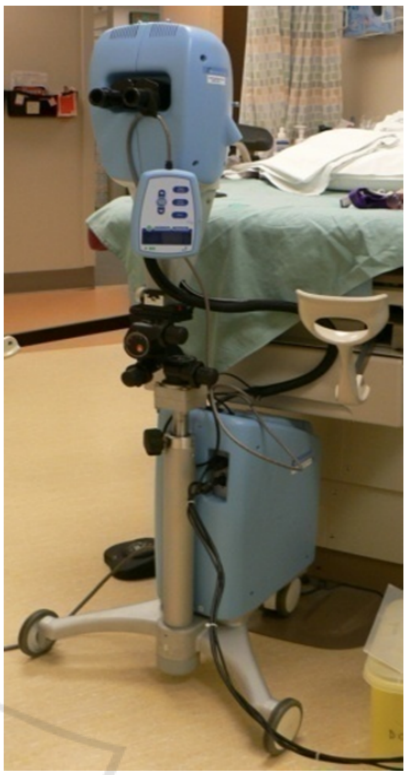

C

Contrast Mode	Illumination (Excitation) Color	Illumination (Excitation) Band (nm)
Reflectance	White	405-680
	Blue	455-465
	Violet	410-430
Fluorescence	Blue	455-465
	Violet	410-430
	Ultraviolet	340-360

Figure 1: This figure shows A) a cartoon of the Multispectral Digital Colposcope (MDC) device, B) a photo of the "in house" device, and C) the table of the illumination colour and excitation.

screening. Morphological, cytological and histo-pathological information can be quantified using fluorescence and reflectance imaging (Nordstrom et al., 2001).

We are interested in developing optical technologies for cervical cancer screening in developing countries. This device was developed to be used as an adjunct to colposcopy (a method for generating a close-up view of the cervix) as an improved guide for biopsy site selection in resource rich countries where screening programs are accessible and robust. This paper reports on the development of a classification algorithm using multispectral image data acquired from MDCs.

2 MATERIALS AND METHODS

2.1 Instrumentation

The MDC is a device that combines whole cervix imaging and a point probe imaging. The analysis presented here only makes use of the whole cervix images. The device acquires a cross polarized white-light illumination image and 2 reflectance and 3 fluorescence images. The system consists of a colposcope, and a colour charge-coupled device (CCD) (MicroPublisher 3.3, QImaging) to capture images. Illumination is provided by a Xenon arc lamp in the base of the device. The lamp provides monochromatic and broadband illumination. The fluorescence excitation light is produced using band-pass filters enclosed in a motorized filter wheel. Figure 1 shows the diagram of the system, a photograph of the system and the specifications of the reflectance and fluorescence excitation light produced by this device. These excitation and emission wavelengths were determined from a previously reported study. (Chang et al., 2002) Previous versions of the device generated an automated diagnosis with 80% sensitivity and 80% specificity for the diagnosis of high-grade SIL (Chang et al., 2002, and Benavides et al., 2003, and Park et al., 2005, and Milbourne et al., 2005 and Park et al., 2008).

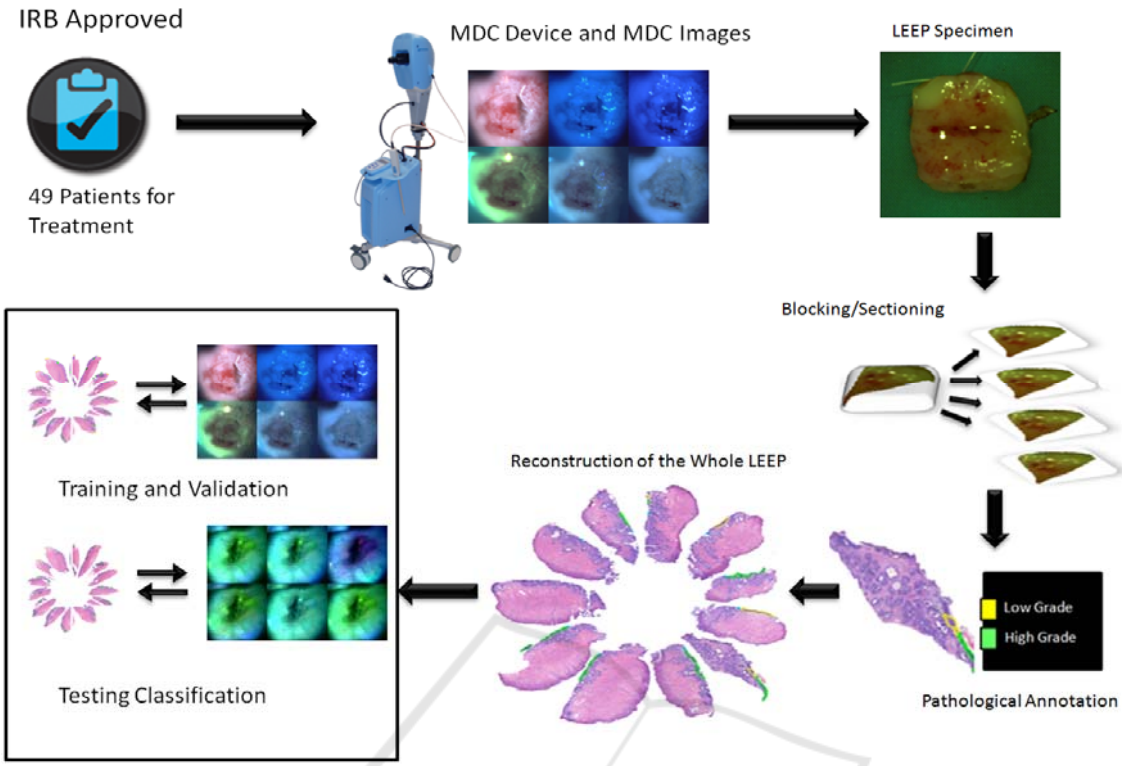

Figure 2: This figure shows the study design. Patients were consented for an IRB-approved study, images were acquired, the Loop Electrical Excision Procedure (LEEP) was carried out, the specimen were processed and annotated, and the dataset was subjected to analysis for training and testing classification.

2.2 Clinical Data

2.2.1 Patients Recruitment and Data Collection

The study protocol was reviewed and approved by the Institutional Review Board (IRB) at the British Columbia Cancer Agency. Eligibility requirements were: 18 years of age or older, high-grade result on a cytologic sample or colposcopically-directed biopsies, and not be pregnant. Each patient was to undergo standard of care Loop Electrical Excision Procedure (LEEP). Participants signed an informed consent for this study.

During colposcopic examination, acetic acid (6%) was applied to the cervix for 2 minutes. Acetic acid enhances the differences in appearance between normal and dysplastic tissue. Six images were taken using the MDC; three reflectance images and three fluorescence images. Sample images are shown in Figure 2. The physician/colposcopist was asked to denote in the white light image which areas were thought to be most abnormal and were the margins or edges of the LEEP specimen were located.

After the application of local anaesthesia, the patients underwent a LEEP. The removed specimen was oriented by the surgeon. The specimen is oriented in reference to a clock face. The most superior part of the specimen was located at the 12 o'clock position; the most inferior was at the 6 o'clock position. The 12 o'clock position was marked on the specimen before going to pathological processing where it was cut into 6-12 pieces each piece's clock position recorded prior to embedding to keep the specimen fragments oriented in the later process.

The LEEP pieces were sectioned and reviewed by a clinical pathologist for final diagnosis and annotated by the study pathologist. Each section was carefully marked identifying areas of low-grade SIL, high-grade SIL, and cancer. Preserving the orientation of each section from each piece helped us to reconstruct the histopathologic map which served as the gold standard for the rest of this study. Figure 2 shows a representation of this process.

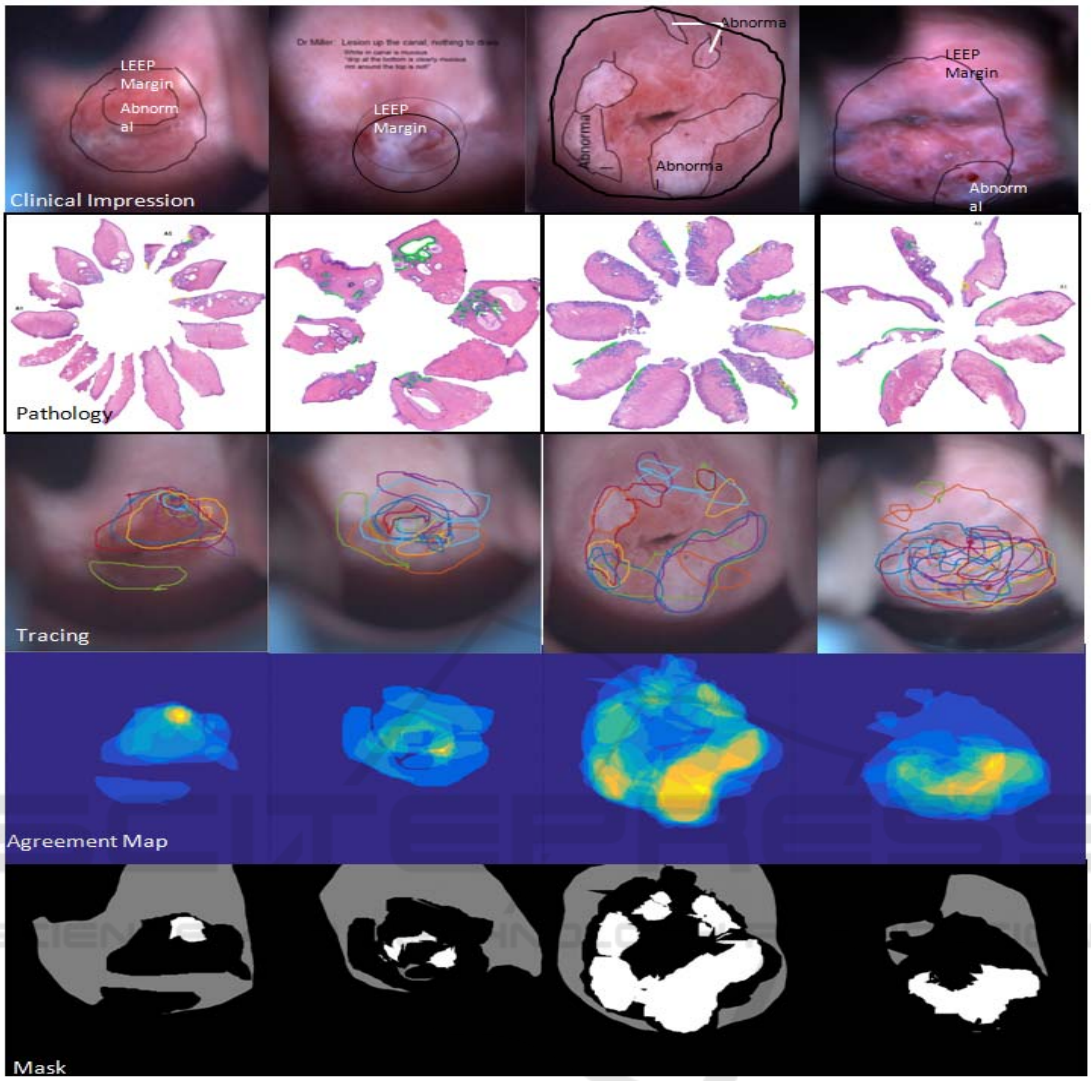

Figure 3: This figure shows four patients results. In each column we present the clinical impression of the colposcopist, the histopathologic map, the tracing by the 11 reviewers, the agreement map, and the mask generated by the calculation of 60% agreement.

2.2.2 Data Preparation and Pre-Processing

Gaussian filters were used to reduce the noise in the images. Image registration was used to correct for image rotation and image translation due to patient motion. We used an automated registration algorithm from MATLAB, "imregister" which was successful in 80% of the cases and for the rest of the images we used manual registration using the cervical os and other landmarks in each image. For the registration process, the white light image was used as our reference.

2.2.3 Image Annotation

A group of 11 experts were tasked with tracing the areas (Region of Interest, ROI) that they believed were associated with high-grade disease based upon only the reconstruction pathology map. The logic to be used in the determination of the ROIs was: 1) search for high-grade (≥CIN2) lesions in the reconstructed pathology map (annotated by the study pathologist), and 2) match the above annotation (if found) to the corresponding areas in the MDC images.

The colposcopic data and MDC images were acquired from 49 patients. Figure 3 shows images and tracings of the ROIs for four of the 49 patients.

The uppermost images show the markings made by the physicians on the white light MDC images. The next row shows the histopathologic maps annotated by the study histopathologist. Areas of CIN 2 and 3 are shown with green markings and HPV changes and CIN 1 are shown with yellow marking. The next row shows the tracings made by the eleven reviewers. The agreement maps are shown as heat-maps in the next row. Finally the last row shows the defined consensus mask used for our analysis.

2.3 Classifier Design

2.3.1 Labelling the MDC Images

Relative to the MDC white light image for our consensus image we considered a location as i) abnormal if 60% of the experts' annotations defined it as ≥CIN2 (we chose 60% agreement in order to have enough positive pixels), ii) "uncertain" if experts' annotation defining it as ≥CIN2 was greater than 0 % but less than 60% , and iii) normal otherwise. Registration relative to the white light image was carried out on all five MDC images, which specifically included the blue and violet reflectance images and the blue, violet and ultraviolet fluorescence images. We then labeled each of the MDC image pixels based on their correspondence to the consensus image.

For our analysis we used a Windows-based approach wherein 10x10-pixel windows were selected from the abnormal/normal areas of MDC images. The corresponding label for this region was the label at the middle of the 10x10 window in the consensus mask. After cleaning the dataset (removing the "uncertain pixels) we obtained 248,960 pixels that were used for classification.

2.3.2 Feature Selection

We used a histogram of the intensities within each window region as our set of features. The reason for this selection was due to the histogram property which conveyed statistical information regarding the image intensity distribution including mean and variance.

2.3.3 Training, Validation, and Test Dataset

We divided our dataset into two sets: 80% were used for training-validation and 20% were used as the test set. We used a boosted tree classifier for our analysis (Windeatt and Ardeshir, 2002). The input of our classifier is the features defined as above (histogram

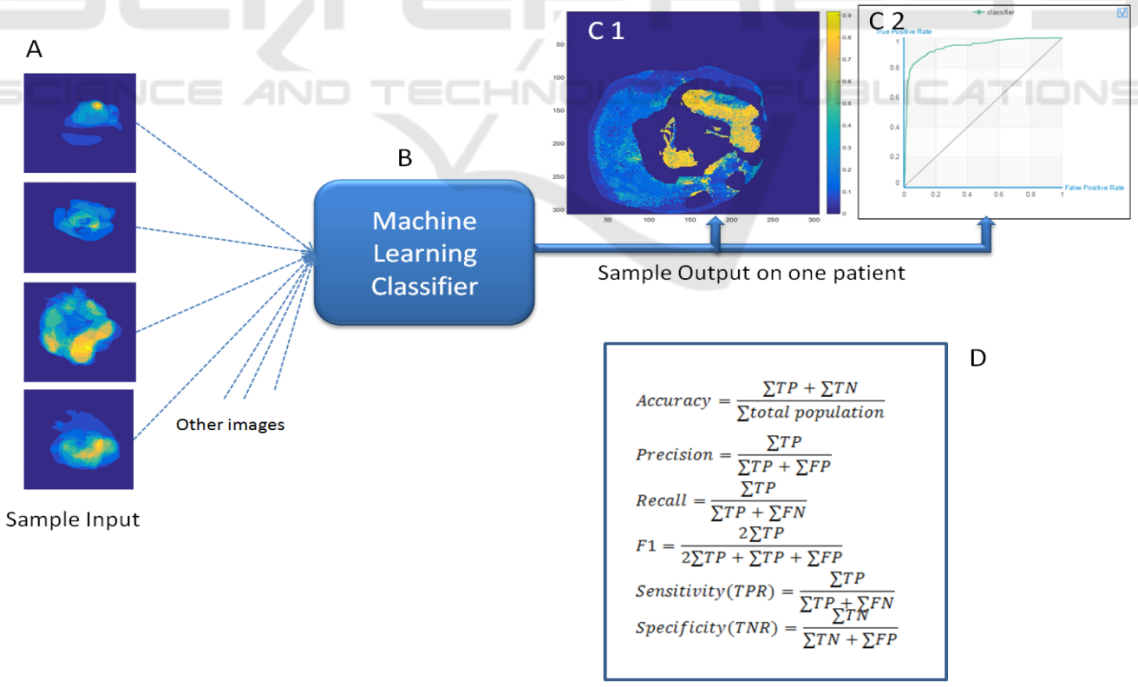

Figure 4: This figure shows the strategy for the analysis. Eighty percent of the data was used to train a classifier, shown in A. The classifier was tested on the remaining data (B). Output from a sample patient is shown in C 1 and 2. The probability of disease in shown in C1 and the Receiver Operating Characteristic (ROC) curve is shown in C2. The formulas in D are used to report the results of the training and test data.

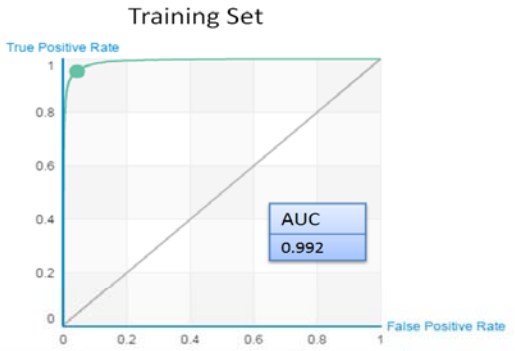

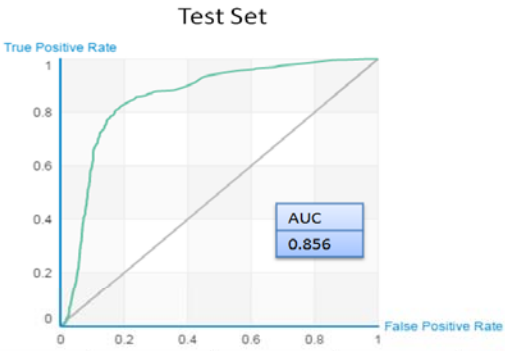

True Positive	False Negative	Accuracy	Precision	Sensitivity (TPR)
24,892	1,228	0.96	0.77	0.96
False Positive	True Negative	Recall	F1 Score	Specificity (TNR)
7,441	165,607	0.95	0.85	0.96

True Positive	False Negative	Accuracy	Precision	Sensitivity (TPR)
2,664	589	0.81	0.24	0.82
False Positive	True Negative	Recall	F1 Score	Specificity (TNR)
8,656	37,882	0.82	0.37	0.81

Figure 5: This figure represents the results of the boosted tree classifier. On the left, we shows the results of the training and validation set using 80% of the data. On the right, we show the results on the test set for the remaining 20% of the data.

of intensities for all MDC images), and the output is the predicted labels for each pixel.

Figure 4 shows the strategy followed for the analysis. As shown in the figure, a probability map and a Receiver Operating Characteristic (ROC) curve can be generated for the pixels of each image. Data on the results of the boosted tree analysis for the entire data set is represented in the sensitivity (recall), specificity, accuracy, precision and an F1 score values.

3 RESULTS

The classification results on both training and test sets are summarized in Figure 5. We obtained 95% sensitivity and 96% specificity when we applied a boosted-tree classifier to the training set and 82% Sensitivity and 81% specificity with the test set. Area Under the Curve (AUC) was 0.99 and 0.86 for training and test set respectively.

4 DISCUSSION

We compared our method with the existing method presented on cervical image data in (Park, et al., 2008) Park group designed an ensemble classifier that consisted of four classifiers, a linear classifier with Euclidian distance, a linear classifier with Mahalanobis distance, a K-nearest neighbour (KNN) classifier with eight neighbours, and a support vector machine with a linear kernel. In This paper the ensemble classifier used only the information in white light images. To compare our method with this method (Park et al., 2008) we implemented their classifier and used only the white light image pixel intensities as input. The result is presented as the red dashed line in Figure 6 suggests near random prediction. When we added other MDC image pixel intensities as input to the ensemble classifier (MDC images), the output ROC curve improved, as shown in Figure 6 by blue dashed line. Our boosted-tree classifier which used MDC images outperformed the method presented from Park group (red dashed line) significantly as shown by the green line in Figure 7.

The strengths of this study are found in the detailed specimen histological review and mapping. The large number of pixels provides a relatively large data set for analysis. Dividing the data into training and test sets allows better estimation of overtraining effects.

Weaknesses of the study include the fact that the histopathologic map does not include detailed section data from every square millimeter of the excised sample. Thus, assumptions were made about the tissue in-between the sections. Another potential study weakness is how the reviewers interpreted the instructions and how accurately they defined the lesions in the consensus map.

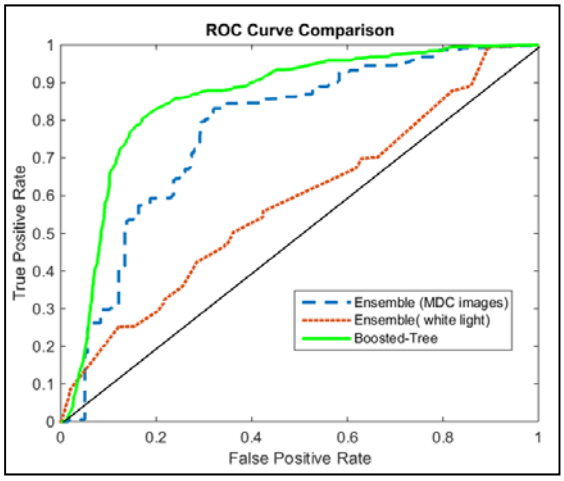

Figure 6: This figure shows the results of the Ensemble (MDC images and only white light) and the Boosted-Tree classifier applied to the test set data.

5 CONCLUSIONS

In this paper, we showed preliminary results from our pilot study for classification of CIN2 or worse tissue from CIN1 or better tissues in cervix. We designed a boosted tree classifier which used the information from the MDC images. We presented promising results that outperformed existing methods applied to cervical images. This study is at an early stage and a larger dataset is needed to validate the effectiveness of this method, we believe this method has the potential to be used as an adjunct to colposcopy and would result in greater accuracy of diagnosis compared to existing methods.

REFERENCES

World Cancer Research, http://www.wcrf.org/int/cancer-facts-figures/data-specific-cancers/cervical-cancer-statistics (13 September 2016).

Nordstrom, et al., 2001 "Identification of cervical intraepithelial neoplasia (CIN) using UV excited fluorescence and diffuse reflectance tissue spectroscopy." *Lasers in Surgery and Medicine 29.2* 118-127.

Chang, et al., 2002, "Optimal excitation wavelengths for discrimination of cervical neoplasia." *IEEE Transactions on Biomedical Engineering 49.10,* 1102-1111.

Benavides, et al., 2003, "Multispectral digital colposcopy for in vivo detection of cervical cancer." *Optics Express 11.10*, 1223-1236.

Park, et al., 2005, "Multispectral digital microscopy for in vivo monitoring of oral neoplasia in the hamster cheek pouch model of carcinogenesis." *Optics Express 13.3,* 749-762.

Milbourne, et al., 2005,"Results of a pilot study of multispectral digital colposcopy for the in vivo detection of cervical intraepithelial neoplasia."*Gynecologic Oncology 99.3*, S67-S75.

Windeatt, and Ardeshir, 2002, Boosted tree ensembles for solving multiclass problems. *In International Workshop on Multiple Classifier Systems (pp. 42-51)*, Springer Berlin Heidelberg.

Park, et al., 2008 "Automated image analysis of digital colposcopy for the detection of cervical neoplasia." *Journal of Biomedical Optics 13.1*, 014029-014029.